PHYSICAL REVIEW C VOLUME 23, NUMBER 4 APRIL 1981

Cross sections and vector analyzing powers for the (d,t) reaction on ^{68}Zn, ^{64}Ni, ^{57}Fe, and ^{53}Cr

J. A. Bieszk* and S. E. Vigdor†
University of Wisconsin, Madison, Wisconsin 53706
(Received 3 November 1980)

Differential cross sections and vector analyzing powers have been measured for $(\vec{d},t)$ reactions induced on ^{68}Zn and ^{64}Ni at $E_d = 12.0$ MeV and on ^{57}Fe and ^{53}Cr at $E_d = 11.0$ MeV. Transitions with $l = 0$, 1, 2, 3, and 4 were observed. The analyzing power measurements for $l = 1$ transitions exhibit a strong, systematic dependence on Q value, in addition to the expected j dependence. Distorted-wave Born approximation calculations generally do not reproduce the $(\vec{d},t)$ analyzing power data quantitatively, but do account qualitatively for the observed Q dependence. A conclusive analysis of data for the odd-A targets, aimed at determining the relative contributions of different j values to mixed-j transitions, has been possible only in those cases where empirical "calibration curves" for the analyzing powers could be drawn from results of single-j transitions of appropriate l, j, and Q. A number of previous spin and parity assignments are confirmed and two new definite assignments are made on the basis of the present data.

[NUCLEAR REACTIONS ^{53}Cr, ^{57}Fe$(\vec{d},d)$, $E=11.0$ MeV; ^{64}Ni, ^{68}Zn$(\vec{d},d)$, $E=12.0$ MeV; measured vector analyzing power $iT_{11}(\theta)$, cross section $\sigma(\theta)$; deduced deuteron optical model parameters. ^{53}Cr, ^{57}Fe$(\vec{d},t)$, $E=11.0$ MeV; ^{64}Ni, ^{68}Zn$(\vec{d},t)$, $E=12.0$ MeV; measured $iT_{11}(E_t,\theta)$, $\sigma(E_t,\theta)$. ^{52}Cr, ^{56}Fe, ^{63}Ni, ^{67}Zn levels deduced spectroscopic factors, J, π. Enriched targets.]

I. INTRODUCTION

Measurements of the vector analyzing power $[iT_{11}(\theta)]$ in $(\vec{d},p)$ reactions are well established as an important tool in nuclear spectroscopy. The strong dependence of $iT_{11}(\theta)$ on the total angular momentum transfer j complements the sensitivity of cross section angular distributions to the orbital angular momentum transfer l. Systematic investigations of $(\vec{d},p)$ reactions have revealed a strong similarity in the measured vector analyzing powers among transitions of a given l and j over a wide range of target mass and Q value.[1] This empirical similarity has proven to be very useful in the analysis of mixed-j transitions encountered either in the case of unresolved final states or in the case of nonzero spin targets, where angular momentum conservation allows a range of j values for a given final state.[2] The relative contributions of the different j values in such cases can often be accurately determined with the use of empirical "calibration curves" drawn from $iT_{11}(\theta)$ measurements for nearby transitions of known l and j, without reliance on theoretical calculations.

Investigations of $(\vec{d},t)$ reactions, while much less extensive than $(\vec{d},p)$ studies, have established a strong j dependence in the vector analyzing power.[3-6] Data for $(\vec{d},t)$ reactions on ^{208}Pb,[3,4] ^{118}Sn,[6] and ^{98}Mo,[6] with the outgoing tritons at energies near or below the Coulomb barrier, are generally well described by the distorted-wave Born approximation (DWBA). The DWBA has been somewhat less successful in reproducing iT_{11} for $(\vec{d},t)$ studies on lighter targets, especially the fp-shell nuclei studied to date, for which the triton energies are typically several MeV above the Coulomb barrier. In addition, the Sn and Mo studies[6] indicate that the $(\vec{d},t)$ vector analyzing power depends considerably more strongly on kinematical factors, e.g., the Q value, than in comparable $(\vec{d},p)$ reactions.

The present work reports $(\vec{d},t)$ measurements on ^{68}Zn and ^{64}Ni at a bombarding energy of $E_d = 12.0$ MeV, and on ^{57}Fe and ^{53}Cr at $E_d = 11.0$ MeV. These data extend $(\vec{d},t)$ systematics on fp-shell nuclei, and we examine in detail the ability of the DWBA to reproduce the vector analyzing power. In particular, the present investigation includes many $l=1$ transitions over a Q-value range of several MeV. Hence, one can systematically study the Q dependence of iT_{11} for $\frac{1}{2}^-$ and $\frac{3}{2}^-$ transitions.

Measurements on the ^{57}Fe and ^{53}Cr targets differ from the $(\vec{d},t)$ studies on even-even targets in that more than one j value is allowed to contribute in transitions to final states of nonzero spin. In principle, cross section measurements determine the l values contributing to a given final state, and measurements of iT_{11} allow a determination of the relative strengths of $l+\frac{1}{2}$ and $l-\frac{1}{2}$ components in the final state configuration. The data for odd-mass targets allow a quantitative evaluation of the analysis of mixed-j $(\vec{d},t)$ transitions using empir-

ical calibration curves taken from the unique-j transitions of the present work. We also report a limited amount of deuteron elastic scattering data for the above targets and energies, taken to aid in the determination of optical model parameters to be used in the DWBA analysis.

II. EXPERIMENTAL DETAILS

The experimental apparatus and procedure have been described in Ref. 6 and will be summarized here. A vector-polarized deuteron beam was produced by the University of Wisconsin Lamb-shift polarized ion source and tandem accelerator. The beam polarization was continuously monitored using a ^{4}He$(\vec{d},d)^4$He polarimeter located behind the scattering chamber used for the $(\vec{d},t)$ measurements. Targets were self-supporting metallic foils enriched in the isotope of interest. Details about the targets are given in Table I.

Deuterons and tritons were detected with four solid-state counter telescopes located on one side of the incident beam. The target was oriented to optimize the resolution of the outgoing tritons. The telescopes were spaced 5° apart and cooled to about -30 °C. An on-line particle identification program[7] was used to distinguish deuterons and tritons. A typical mass spectrum can be seen in Fig. 1 of Ref. 6. Triton spectra for each target nucleus are shown in Fig. 1. The resolution was approximately 50 keV full width at half maximum (FWHM) for the ^{64}Ni and ^{68}Zn targets and approximately 100 keV FWHM for the ^{57}Fe and ^{53}Cr targets.

TABLE I. Targets used in the $(\vec{d},t)$ study.

Target	Enrichment	Thickness
^{64}Ni	97.9% in ^{64}Ni	0.93 mg/cm^2
^{68}Zn	98.5% in ^{68}Zn	1.1 mg/cm^2
^{57}Fe	78.0% in ^{57}Fe	2.46 mg/cm^2
^{53}Cr	86.4% in ^{53}Cr	~3.0 mg/cm^2

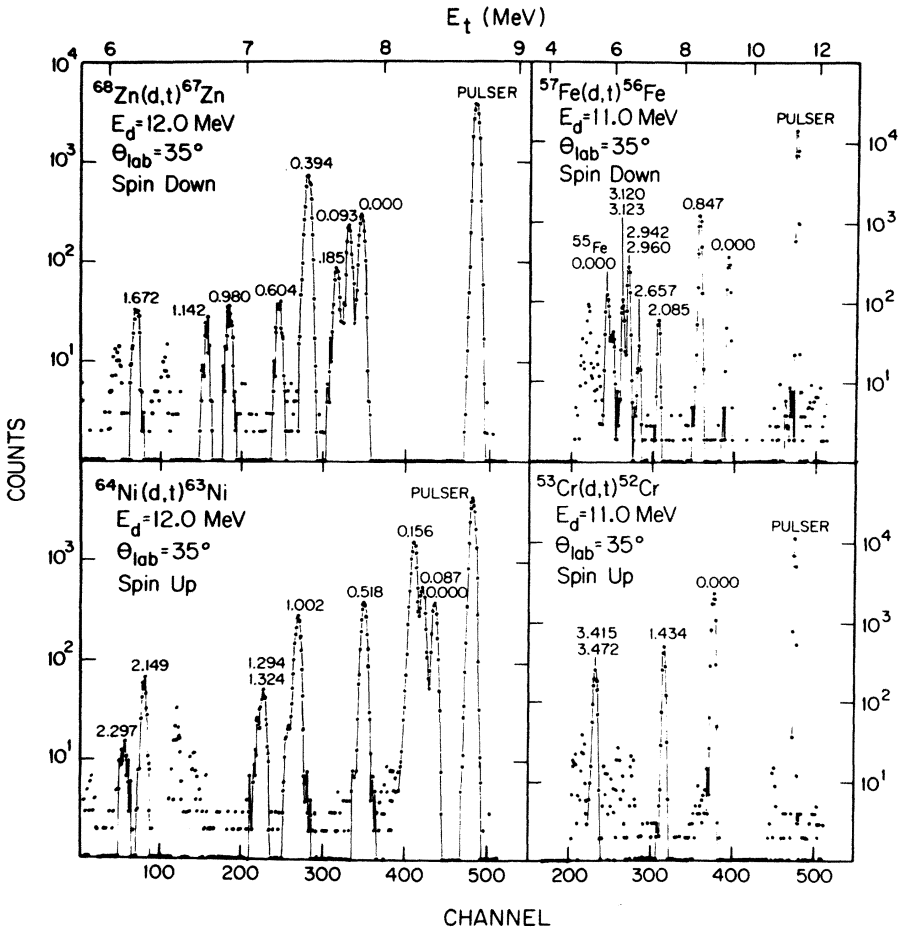

FIG. 1. Representative energy spectra for the $(\vec{d},t)$ reaction on ^{68}Zn, ^{64}Ni, ^{57}Fe, and ^{53}Cr. Peaks are labeled by the excitation energy in MeV (taken from Refs. 12–15) of the level populated in the residual nucleus.

Areas under overlapping peaks in the tritons spectra were determined with a peak-fitting program employing a model peak shape based on the observed shape of a large isolated peak. Details of the determination of cross sections and vector analyzing powers are given in Ref. 6.

The error bars on the experimental results presented in the following sections include uncertainties arising from counting statistics, background subtraction, and peak fitting, but do not include absolute normalization uncertainties. The magnitude of all measured analyzing powers may be in error by a factor between 0.97 and 1.03 because of the 3% uncertainty in the vector analyzing power of the ^{4}He($\vec{d}$,d) polarimeter. Possible systematic errors in the beam integration and in the elastic scattering cross section assumed at the angles of the left-right monitor detectors give rise to an overall normalization uncertainty of approximately ±5% for all absolute cross section results reported here. Additional details about uncertainties in the measurements can be found in Ref. 6.

III. ELASTIC SCATTERING RESULTS AND ANALYSIS

Differential cross sections and vector analyzing powers for deuteron elastic scattering from ^{68}Zn, ^{64}Ni, ^{57}Fe, and ^{53}Cr were measured over limited angular ranges. These data were not intended to be the subject of an exhaustive optical model analysis, but rather allowed a search for small improvements to potentials already available for neighboring nuclei and/or energies (Ref. 8 for ^{64}Ni and ^{68}Zn, Ref. 2 for ^{53}Cr and ^{57}Fe). The measurements and optical model fits are shown in Fig. 2. The explicit form of the optical potentials used is described by Schwandt and Haeberli.[9] The analysis was performed with the search code

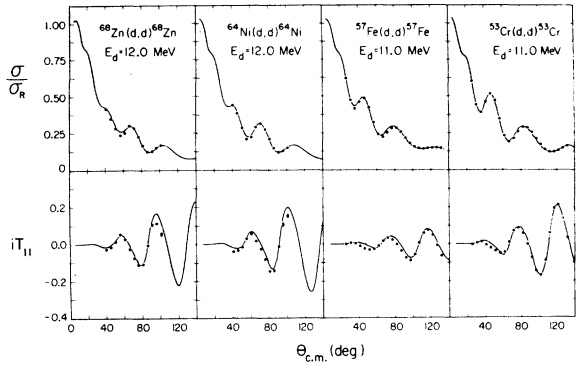

FIG. 2. Angular distributions of the ratio of experimental to Rutherford cross section and of the vector analyzing power for the ^{68}Zn($\vec{d}$, d)^{68}Zn, ^{64}Ni($\vec{d}$, d)^{64}Ni, ^{57}Fe($\vec{d}$, d)^{57}Fe, and ^{53}Cr($\vec{d}$, d)^{53}Cr reactions. The curves are optical model fits obtained with the potentials labeled "a" in Table II.

TABLE II. Optical model parameters (all potential strengths are in MeV; all lengths are in fm).

Nucleus	Particle	Energy (MeV)	Parameter set	V_0	r_0	a_0	W_V	W_D	r_I	a_I	V_{so}	r_{so}	a_{so}	r_C
^{64}Ni	d	12.00	a	109.98	1.05	0.86		15.21	1.351	0.711	8.46	0.706	0.414	1.3
^{64}Ni	d	12.00	b	106.53	1.05	0.86		13.63	1.43	0.71	7.0	0.75	0.5	1.3
^{63}Ni	t	8.62[f]	c	162.82	1.2	0.72	30.93		1.4	0.84	2.5	1.2	0.72	1.3
^{63}Ni	t	8.62	d	165.40	1.2	0.72	34.0		1.4	0.84	2.5	1.2	0.72	1.3
^{63}Ni	t	8.62	e	168.00	1.2	0.65	13.5		1.6	0.87	6.0	1.15	0.51	1.3
^{68}Zn	d	12.00	a	111.87	1.05	0.86		14.92	1.341	0.738	7.38	0.704	0.486	1.3
^{68}Zn	d	12.00	b	107.30	1.05	0.86		13.09	1.43	0.717	7.0	0.75	0.50	1.3
^{67}Zn	t	8.06[f]	c	162.89	1.2	0.72	31.70		1.40	0.84	2.5	1.2	0.72	1.3
^{67}Zn	t	8.06	d	165.40	1.2	0.72	34.0		1.40	0.84	2.5	1.2	0.72	1.3
^{67}Zn	t	8.06	e	168.00	1.2	0.65	13.5		1.6	0.87	6.0	1.15	0.51	1.3
^{57}Fe	d	11.00	a	82.01	1.23	0.772		17.60	1.345	0.725	4.06	0.90	0.60	1.3
^{56}Fe	t	9.47[f]	c	162.90	1.20	0.72	34.93		1.40	0.84	2.5	1.2	0.72	1.3
^{53}Cr	d	11.00	a	83.22	1.23	0.772		15.72	1.377	0.690	5.16	0.90	0.60	1.3
^{52}Cr	t	9.43[f]	c	162.90	1.2	0.72	34.43		1.40	0.84	2.5	1.2	0.72	1.3

[a] Parameters determined from an analysis of the present elastic scattering cross section and vector analyzing power data.

[b] Parameters determined from the global analysis of Lohr and Haeberli (Ref. 8).

[c] Parameters determined from the global analysis of Becchetti and Greenlees (Ref. 11). (The energy dependence of these parameters is given in Ref. 11.)

[d] Parameter set used to investigate the sensitivity of DWBA calculations to triton optical model parameters.

[e] Parameters determined from an analysis of the elastic scattering of polarized tritons on ^{90}Zr (Ref. 20).

[f] Energy of the ground state triton group.

SNOOPY 2.[10] In all searches on the deuteron optical model parameters, the Coulomb radius and volume absorption were held fixed at $r_C = 1.3$ fm and $W_v = 0.00$ MeV. In fitting the ^{68}Zn and ^{64}Ni data, the radius and diffuseness of the real central well were fixed at their initial values of 1.05 and 0.86 fm, respectively, with the remaining seven parameters varied to obtain the fits in Fig. 2. For the ^{57}Fe and ^{53}Cr analyses, r_{so} and a_{so} were fixed at their initial values. The central potential depths and geometries and the depth of the spin-orbit potential were varied to achieve optimum fits. The final optical model parameters are given in Table II. The changes from the starting parameters are found to be small for ^{68}Zn and ^{64}Ni, but in some cases substantial for ^{57}Fe and ^{53}Cr. For all targets, however, differences in the DWBA calculations for $(\vec{d},t)$ transitions between the starting and the final deuteron optical model parameters are small and do not qualitatively change the conclusions of the present work.

Examining the elastic data, one finds that the Zn and Ni data are quite similar. The magnitude of iT_{11} for ^{57}Fe is approximately half that for the ^{64}Ni and ^{53}Cr data. A similar difference in the amplitude of iT_{11} for ^{53}Cr and ^{57}Fe has also been found at 10 MeV (Ref. 2). A discussion of this result and the possible effect on the optical potential parameters is given in Ref. 2 and will not be pursued further here.

IV. RESULTS AND ANALYSIS OF THE $(\vec{d},t)$ REACTIONS

A. The $l=1$ transitions with unique j value

1. Empirical systematics of the vector analyzing power

Figures 3–5 contain the data for most of the $l=1$ transitions studied in the present work. The spins of the final states are known from previous work,[12–15] except for the 2.149 MeV level in ^{63}Ni. For the latter state the data to be discussed below clearly indicate a $\frac{3}{2}^-$ assignment.

The basic conclusion from these data is that while the j dependence of the analyzing power is as pronounced as in $(\vec{d},p)$ reactions on intermediate-weight nuclei, the sensitivity to kinematic conditions is much greater in the $(\vec{d},t)$ reactions. Figure 3 compares the analyzing power angular distributions for three pairs of $\frac{1}{2}^-$ and $\frac{3}{2}^-$ transitions, the two transitions in each pair having nearly the same Q value. Note that $iT_{11}(\theta)$ for $\frac{1}{2}^-$ states is generally larger in magnitude than $iT_{11}(\theta)$ for $\frac{3}{2}^-$ states, a result reminiscent of the relation

$$\frac{[iT_{11}(\theta)]_{l+1/2}}{[iT_{11}(\theta)]_{l-1/2}} = \frac{-l}{l+1}, \tag{1}$$

which is valid only in the absence of spin-dependent forces.[16] As Q changes, the oscillations in $iT_{11}(\theta)$ shift rapidly in phase, but to nearly the same extent for both j values. So long as we compare transitions of similar Q value, the $\frac{1}{2}^-$ and $\frac{3}{2}^-$ analyzing powers oscillate predominantly out of phase with one another. However, the phase of the oscillations for a $\frac{1}{2}^-(\frac{3}{2}^-)$ transition with $Q \approx 1.5$ MeV is very similar to that for a $\frac{3}{2}^-(\frac{1}{2}^-)$ transition with $Q \approx 4.4$ MeV.

The Q dependence of the $\frac{1}{2}^-$ transitions is examined in more detail in Fig. 4. As Q becomes more negative, the oscillations in the $\frac{1}{2}^-$ analyzing

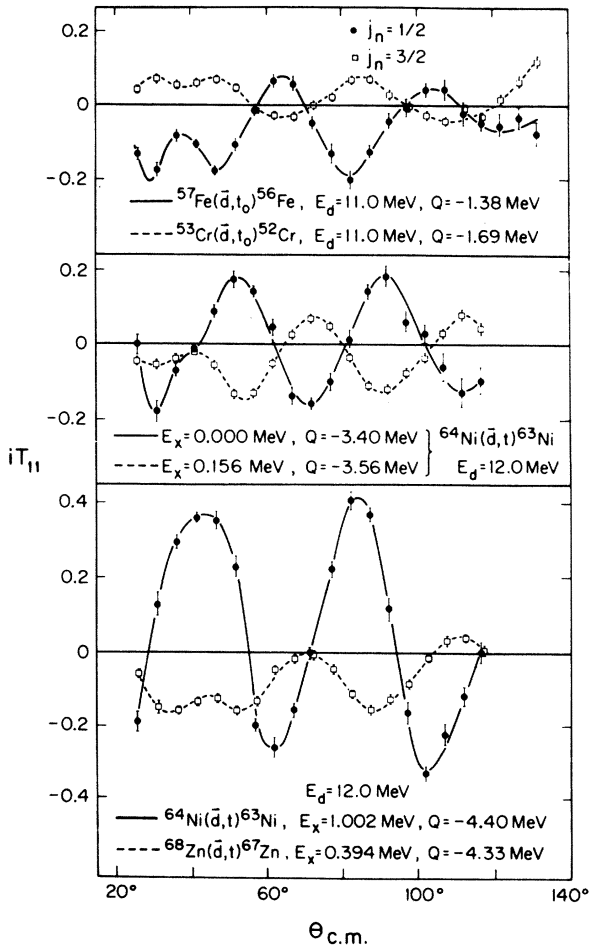

FIG. 3. A comparison of the measured analyzing power distributions for three pairs of $\frac{1}{2}^-$ and $\frac{3}{2}^-$ transitions. The transitions in each pair have approximately the same Q value. The curves are intended to guide the eye.

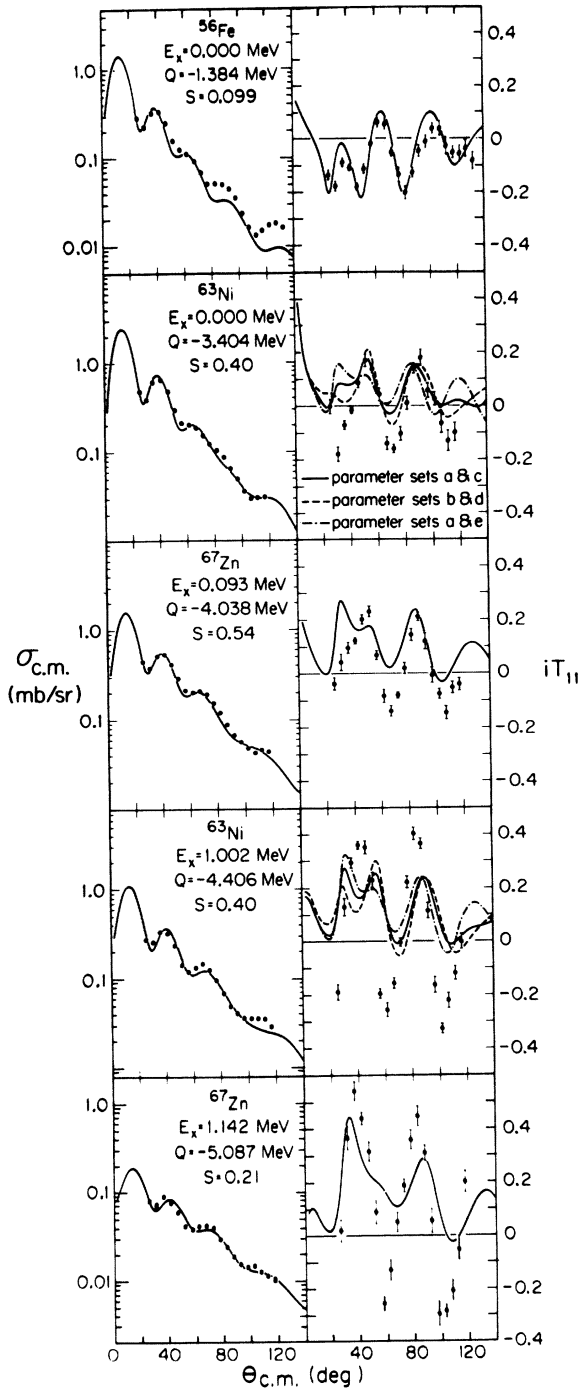

FIG. 4. Angular distributions of the differential cross section and of the vector analyzing power for $\frac{1}{2}^-(\vec{d},t)$ transitions, arranged (from top to bottom) in order of decreasing Q value. The solid and broken curves are the results of DWBA calculations employing the optical model parameters of Table II. Note the inability of the DWBA to reproduce quantitatively the empirical Q dependence in $iT_{11}(\theta)$. The spectroscopic factor S obtained by normalizing the DWBA cross section calculation to the forward-angle measurements is specified for each transition.

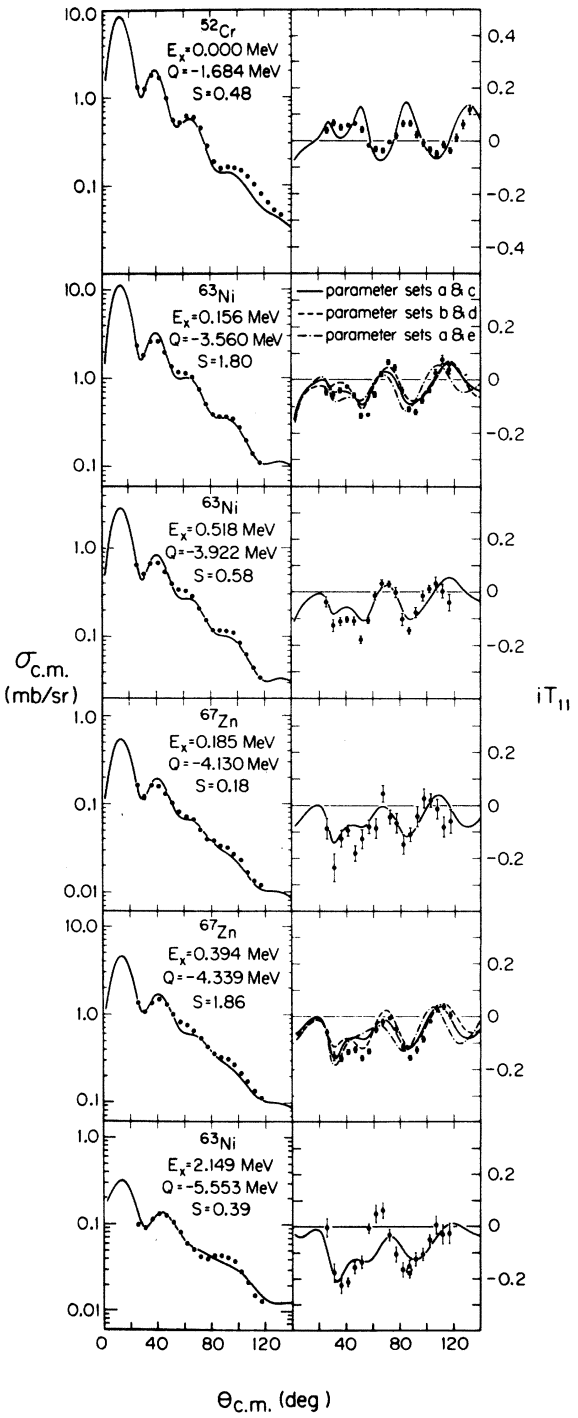

FIG. 5. Angular distributions of the differential cross section and of the vector analyzing power for $\frac{3}{2}^-(\vec{d},t)$ transitions, arranged in order of decreasing Q value. The solid and dashed curves are the results of DWBA calculations employing the optical model parameters of Table II.

powers move steadily toward more forward angles and the analyzing power increases in magnitude, especially in the positive-going excursions. While the significant change observed between the ^{57}Fe$(\vec{d},t)$ and ^{64}Ni$(\vec{d},t)$ ground-state analyzing powers (top two frames) might be attributed in part to changes in target mass and bombarding energy, there are several reasons for believing that it reflects mainly the 2 MeV difference in Q value. First, the extent of the angular shift in the oscillation pattern is consistent with that observed for the 1 MeV change in Q value between ^{64}Ni$(\vec{d},t)$ transitions to the ground and 1.002 MeV states of ^{63}Ni. Second, we have made measurements for ^{57}Fe$(\vec{d},t_0)$ at $E_d=12.0$ MeV between 20° and 85° which show that the angular distribution of iT_{11} remains essentially unchanged from 11.0 MeV, except for a slight increase in the amplitude of the oscillations. In addition, DWBA calculations for hypothetical $\frac{1}{2}^-$ transitions in ^{57}Fe$(\vec{d},t)$ (to be discussed below, see Fig. 6) predict a Q dependence similar to that observed.

Data for the $\frac{3}{2}^-$ transitions are presented in Fig. 5. As seen for the $\frac{1}{2}^-$ states, the oscillations in $iT_{11}(\theta)$ move forward, and their amplitude increases, with decreasing Q value, although the amplitude variation is not as dramatic as in Fig. 4. A simple average of the analyzing power over the angular distribution shifts nearly linearly with

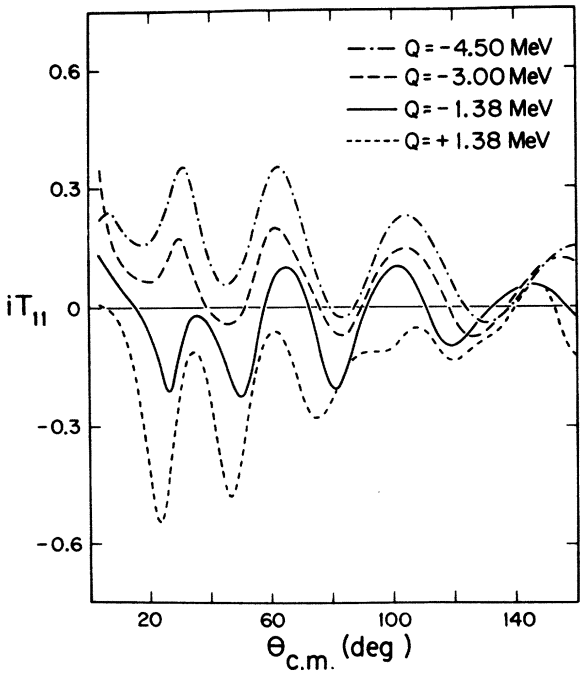

FIG. 6. Results of DWBA calculations predicting the Q dependence of the vector analyzing power for $\frac{1}{2}^-$ transitions using hypothetical Q values in the ^{57}Fe$(\vec{d},t)^{56}$Fe reaction.

Q value for both $\frac{1}{2}^-$ and $\frac{3}{2}^-$ transitions, becoming more positive as Q decreases for $\frac{1}{2}^-$ and more negative for $\frac{3}{2}^-$.

The data alone thus demonstrate that spin determinations based solely upon comparison of $(\vec{d},t)$ measurements for different transitions may not always be reliable (e.g., compare the results in Fig. 3 for the $\frac{1}{2}^-$ transition to the ^{56}Fe ground state with those for the $\frac{3}{2}^-$ transition to the 0.394 MeV state in ^{67}Zn). At least for triton energies not too far above the Coulomb barrier, empirical comparisons of iT_{11} data are useful only for $(\vec{d},t)$ transitions of quite similar Q value (and probably also of similar target mass). While the present measurements go a long way toward establishing systematic empirical "calibration" curves for $l=1$ $(\vec{d},t)$ reactions on intermediate-weight nuclei, extrapolation from these curves into other mass, energy, or Q-value regions is dangerous.

2. *Comparison with DWBA calculations*

The solid curves in Figs. 4 and 5 are DWBA calculations using the elastic deuteron optical model parameters from Table II (set a) and the triton parameters (set c) of Becchetti and Greenless.[11] The spectroscopic factors determined by normalizing these calculations to the cross sections measured at the most forward angles are specified in the figures. The Ni and Zn cross section angular distributions are well reproduced, but the Fe and Cr cross sections are underestimated at larger angles. The calculations agree well with the analyzing power measurements for the $\frac{3}{2}^-$ transitions at all Q values, but exhibit deviations from the $\frac{1}{2}^-$ analyzing powers which increase as Q decreases. Difficulties in reproducing $iT_{11}(\theta)$ for $\frac{1}{2}^-$ states have also been found in ^{58,60,62}Ni$(\vec{d},t)$ (Ref. 17), ^{64}Zn$(\vec{d},t)$ (Ref. 18), and ^{70}Ge$(\vec{d},t)$ (Ref. 19) studies.

The effect on these discrepancies of variations in the deuteron and triton optical model parameters were investigated. DWBA calculations were made with an alternate set of deuteron and triton parameters (sets b and d in Table II) and are presented for representative transitions as dashed curves in Figs. 4 and 5. Some improvement can be obtained for individual transitions, but no overall quantitative improvement was found in the description of the Q dependence of iT_{11}.

DWBA calculations were also made using elastic deuteron parameters (set a) and the Los Alamos triton parameters (set e) determined from elastic scattering of 17 MeV tritons from ^{90}Zr.[20,21] Sample calculations are shown as dot-dashed curves in Figs. 4 and 5. These calculations are similar to the previous ones and again do not describe the Q dependence of the analyzing power any more

quantitatively.

The DWBA does appear to explain at least the qualitative trends of the analyzing power data. Calculations were made for the ^{57}Fe$(d,t)^{56}$Fe reaction for $\frac{1}{2}^-$ transitions with hypothetical Q values, using elastic deuteron parameters and Becchetti-Greenlees triton parameters. The energy dependence of the triton parameters required the use of somewhat different central potential depths for each Q value. Results of these calculations are shown in Fig. 6. The calculated analyzing power is predominantly negative at positive Q values and positive at large negative Q values. [Such a sign change in $(\vec{d},t)$ analyzing powers for $j=l-\frac{1}{2}$ transitions is to be expected over this Q-value range for Coulomb distortions alone, see Ref. 22. However, the oscillations in $iT_{11}(\theta)$ and their shift in phase with Q depend on the presence of nuclear distortions as well.] In the Q-value region spanning the range encountered in the present work, the calculations exhibit sign changes and shifts in phase roughly similar to those actually observed.

It is interesting that the DWBA calculations reproduce the analyzing powers better for the $\frac{3}{2}^-$ than for the $\frac{1}{2}^-$ transitions (see Figs. 4 and 5). This observation suggests an inadequate treatment in the DWBA calculations of some aspect of the spin-dependent distortions, since in the absence of such distortions iT_{11} would be simply related for $\frac{1}{2}^-$ and $\frac{3}{2}^-$ transitions of similar Q. One possible spin-dependent effect that is ignored in the usual DWBA calculations for the (d,t) reactions arises from the deuteron and triton D states. Calculations of $iT_{11}(\theta)$ for the 0.00 and 0.156 MeV states in ^{63}Ni were made using the program DTCODE,[23] which includes D-state terms in the local energy approximation. The results of these calculations reveal that the D-state effects are larger for the $\frac{3}{2}^-$ than for the $\frac{1}{2}^-$ transitions, but that in both cases they are very much smaller than the discrepancies observed between the data and the DWBA calculations in Figs. 4 and 5.

B. Single transitions with $l \neq 1$

The measurements and DWBA calculations for the two $l=3$ transitions studied (both known to have $j=\frac{5}{2}$ from previous work) are shown in Fig. 7. Note that since these transitions have similar Q values, the data are quite similar for the two states. The cross section data are reasonably reproduced by the calculations, but there are substantial differences between the calculated and the measured $\frac{5}{2}^-$ analyzing powers, most notably in the amplitude of the oscillations. In fact, the iT_{11} comparison for the ^{63}Ni 0.087 MeV state indicates only a slight preference for the $j=\frac{5}{2}$ (over the $j=\frac{7}{2}$) DWBA calculation at forward angles. The ^{67}Zn 0.000 MeV data show a more definite preference for the $j=\frac{5}{2}$ assignment at forward angles. In both cases, the oscillations in the $\frac{5}{2}^-$ calculations are approximately in phase with the data, while the $\frac{7}{2}^-$ calculations are generally out of phase with the measurements. Examining previous (d,t) studies, one finds that the differences between measured and calculated $\frac{5}{2}^-$ vector analyzing powers are somewhat larger here than observed in ^{58,60,62}Ni$(\vec{d},t)$ (Ref. 17), ^{64}Zn$(\vec{d},t)$ (Ref. 18), and ^{70}Ge$(\vec{d},t)$ (Ref. 19) investigations.

Measurements and calculations for the two $l=2$ transitions studied in this work are presented in Fig. 8. Both of these have been previously identified, at least tentatively, as $\frac{5}{2}^+$ transitions.[12,13] The measured analyzing powers for the two transitions are indeed quite similar (at all angles forward of 100°), but the cross section angular distributions differ substantially in their oscillatory behavior and in the average rate of falloff with angle. The sizable discrepancies observed in Fig. 8 between the calculated and measured cross sections for the 0.980 MeV level in ^{67}Zn are reminiscent of the difficulties reported by Borsaru *et al.*[24] in reproducing ^{68}Zn(d,t) data for this state. The $l=2$ assignment, however, is strongly supported by (d,p) studies[25-27] (unless, of course, there is a doublet at this energy which has never yet been resolved). The cross section agreement is considerably better for the 2.297 MeV state in

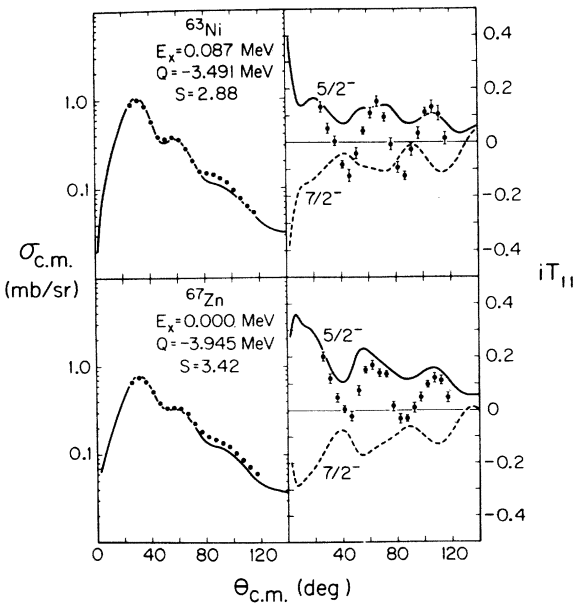

FIG. 7. Angular distributions of the differential cross section and of the vector analyzing power for $\frac{5}{2}^-(\vec{d},t)$ transitions. The solid and dashed curves are the results of DWBA calculations employing the optical model parameters of Table II.

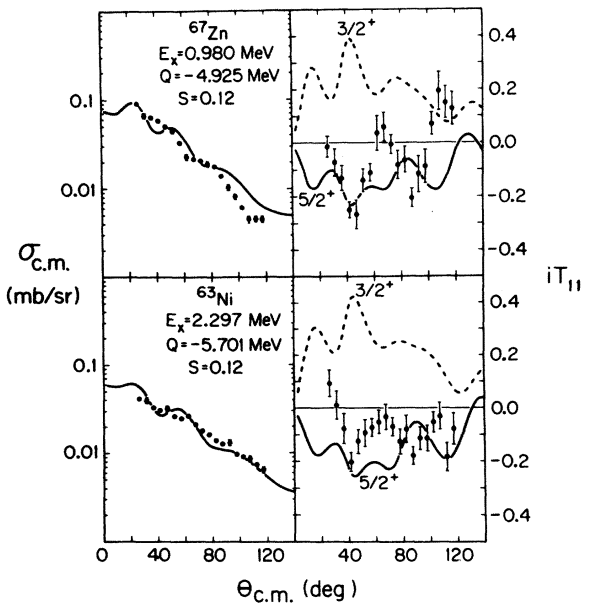

FIG. 8. Angular distributions of the differential cross section and of the vector analyzing power for $\frac{5}{2}^+(\vec{d},t)$ transitions. The solid and dashed curves are the results of DWBA calculations employing the optical model parameters of Table II.

^{63}Ni. Although the calculations fall far short of quantitatively reproducing the analyzing power measurements for the $l=2$ transitions, still the agreement is sufficient in both cases to strongly support a $\frac{5}{2}^+$, as opposed to a $\frac{3}{2}^+$, assignment.

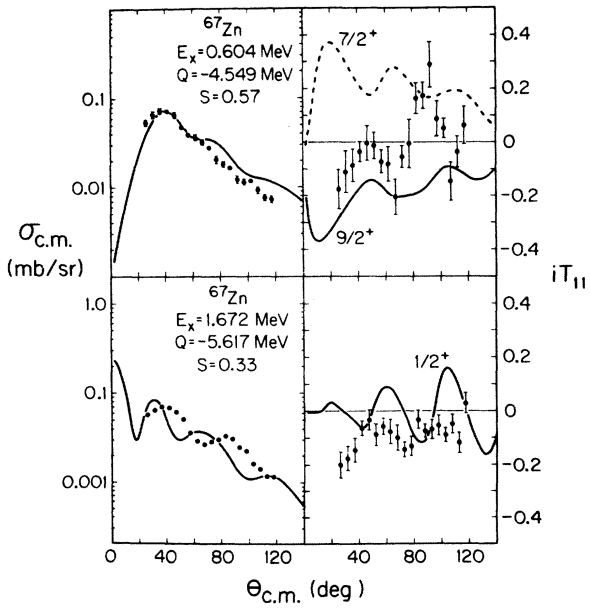

FIG. 9. Angular distributions of the differential cross section of the vector analyzing power for the isolated $\frac{9}{2}^+$ and $\frac{1}{2}^+(\vec{d},t)$ transitions studied. The solid and dashed curves are the results of DWBA calculations employing the optical model parameters of Table II.

The single $l=0$ transition studied in the present work is represented in Fig. 9. The 1.672 MeV level in ^{67}Zn is known to be a $3s_{1/2}$ state since $l=0$ transitions to this level have been observed in ^{66}Zn(d,p) reactions.[25-27] This state had been previously identified as a $2s_{1/2}$ state in the (d,t) work of Borsaru *et al.*[24] The present cross section and iT_{11} data are poorly reproduced by the DWBA calculations.

The only isolated $1g_{9/2}$ transition observed in this work is the 0.604 MeV level in ^{67}Zn. The data for this state, displayed in Fig. 9, are not very well described by the DWBA calculation. Nonetheless, the comparison with DWBA does support the previous $\frac{9}{2}^+$ assignment to this state.[12]

C. Unresolved and mixed-j transitions

Vector analyzing power measurements have proven very useful in $(\vec{d},p)$ reactions for distinguishing the relative contributions from different j values to transitions leading to unresolved final states, or to transitions between two states with nonzero spin.[2] A similar application of iT_{11} measurements has been reported for the ^{37}Cl$(\vec{d},t)^{36}$Cl reaction.[28] One must expect only limited success in the analysis of the present multiple-j $(\vec{d},t)$ transitions, given the above results for single-j transitions—namely, the strong Q dependence observed for the analyzing powers and their generally poor quantitative description by DWBA calculations. In light of these problems, we confine our attention here to three cases in ^{57}Fe(d,t) of unresolved or mixed-j transitions where previous work, together with the present cross section results, indicate possible contributions only from l and j values for which empirical $iT_{11}(\theta)$ calibration curves can be drawn from measurements for single-j transitions of appropriate Q value.

As an example, consider the transition (with $Q=-4.04$ MeV) from ^{57}Fe $(J^\pi=\frac{1}{2}^-)$ to the 2.657 MeV state in ^{56}Fe $(J^\pi=2^+$, Ref. 14), which can proceed in principle via pickup of either a $\frac{3}{2}^-$ or a $\frac{5}{2}^-$ neutron. Calibration curves for the analyzing power are available from the ^{64}Ni$(\vec{d},t)^{63}$Ni 0.518 MeV transition $(\frac{3}{2}^-$, $Q=-3.92$ MeV) and from the ^{68}Zn$(\vec{d},t)^{67}$Zn ground-state transition $(\frac{5}{2}^-$, $Q=-3.95$ MeV). The measured $iT_{11}(\theta)$ for the transition to the ^{56}Fe 2.657 MeV state is compared to these calibration curves, and the measured cross sections are compared to $\frac{3}{2}^-$ $(l=1)$ and $\frac{5}{2}^-$ $(l=3)$ DWBA calculations, in Fig. 10. Both the cross section and analyzing power measurements are well explained under the assumption of a pure $\frac{3}{2}^-$ pickup. The ^{57}Fe(d,t) study of Daehnick[29] also indicated no

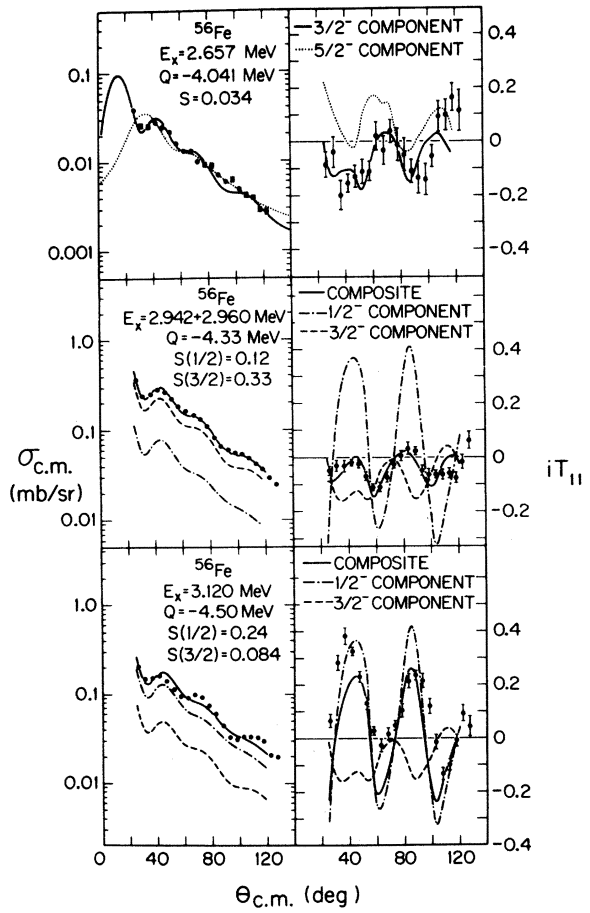

FIG. 10. Angular distributions of the differential cross section and of the vector analyzing power for three cases in the ^{57}Fe$(\vec{d},t)^{56}$Fe reaction of unresolved or (potentially) mixed-j transitions. Empirical calibration curves from the measurements for single-j transitions of appropriate l, j, and Q values are used in the analysis of $iT_{11}(\theta)$, while DWBA calculations are used for the cross sections.

significant $l=3$ contribution to this state.

The analysis of the unresolved transitions (with $Q=-4.33$ MeV) to the 2.942 and 2.960 MeV states in ^{56}Fe (Fig. 10) demonstrates the applicability of the analyzing power measurements to a *quantitative* determination of relative spectroscopic factors for different j values. These two states have been previously resolved in the (d,t) study by Daehnick,[29] whose cross section measurements indicated pure $l=1$ transitions to both. This conclusion is confirmed by the excellent agreement between $l=1$ DWBA calculations and the present cross section measurements (see Fig. 10). An acceptable fit to the measured analyzing powers can be obtained only with a combination of $\frac{1}{2}^-$ and $\frac{3}{2}^-$ transitions, using calibration curves from data for the ^{63}Ni 1.002 MeV ($\frac{1}{2}^-$, $Q=-4.40$ MeV) and ^{67}Zn 0.394 MeV ($\frac{3}{2}^-$, $Q=-4.34$ MeV) levels. Such a mixture is consistent with the previous spin-parity assignments[14] of 0^+ for the 2.942 MeV state and 2^+ for the 2.960 MeV state. By adjusting the spectroscopic factors (S) for the two transitions, we achieve an optimum fit to $\sigma(\theta)$ and $iT_{11}(\theta)$ (see Fig. 10) at values $s(\frac{1}{2}^-)=0.12$, $s(\frac{3}{2}^-)=0.33$, in excellent agreement with the values $s(2.94)=0.11$, $s(2.96)=0.32$ obtained by Daehnick (at $E_d=11.7$ MeV) when the states were resolved. In view of the enormous difference between the $\frac{1}{2}^-$ calibration curve used in analyzing these transitions and the $\frac{1}{2}^-$ analyzing power distribution observed for the ^{57}Fe$(\vec{d},t_0)$ transition (Fig. 4), this excellent agreement in spectroscopic factors and the high quality of fit to $iT_{11}(\theta)$ for the 2.942 +2.960 MeV states (Fig. 10) provide further evidence that the strong variation of iT_{11} seen in Figs. 3–5 arises predominantly from a dependence on Q, rather than on target or bombarding energy.

Reference 14 reports states in ^{56}Fe at 3.120 and 3.123 MeV with spin-parity assignments of (1^+) (tentative) and 4^+, respectively. A (d,t) transition to the latter level would involve either $\frac{7}{2}^-$ or $\frac{9}{2}^-$ transfer, neither of which have appropriate iT_{11} calibration curves available. As seen in Fig. 10, however, the cross section measurements for the peak at this excitation are reasonably well described by a pure $l=1$ calculation, with the agreement deteriorating upon admixture of an appreciable $l=3$ or $l=5$ contribution. The implication that the 3.123-MeV level is at most, weakly populated is consistent with the conclusion of Daehnick's previous ^{57}Fe(d,t) study.[29] We therefore have analyzed the iT_{11} measurements for this case as a $\frac{1}{2}^- - \frac{3}{2}^-$ mixture, using the same calibration curves as for the 2.942 + 2.960 MeV states. [Note that in a mixed-j transition to a single state, contributions from different j values corresponding to the same l (e.g., $\frac{1}{2}^-$ and $\frac{3}{2}^-$) add *incoherently* in the overall cross section and analyzing power; see Satchler, Ref. 16.] The quality of fit to $iT_{11}(\theta)$ is not quite as good as in the latter case, but still clearly indicates (see Fig. 10) that the transition to the 3.120-MeV state is dominated by $\frac{1}{2}^-$ pickup. This observation constrains the spin and parity of this state to be either 0^+ or 1^+. The 1^+ assignment is weakly favored since the quality of fit to $iT_{11}(\theta)$ is somewhat improved by the admixture of a small $\frac{3}{2}^-$ component.

In the present experiment, data were also obtained for a number of other unresolved or multiple-j transitions. The analysis for these transitions was inconclusive because of a lack of empirical iT_{11} calibration curves for some of the possible contributing j values. This problem is espec-

ially serious for $^{53}Cr(\vec{d},t)$, since the target spin parity is $\frac{3}{2}^-$, allowing up to four different angular momentum transfers to contribute to the population of single ^{52}Cr states with $J > 2$.

V. SUMMARY AND CONCLUSIONS

We have measured differential cross sections and vector analyzing powers for $(\vec{d},t)$ transitions on targets of ^{68}Zn, ^{64}Ni, ^{57}Fe, and ^{53}Cr, involving orbital angular momentum transfers $l=0$, 1, 2, 3, and 4. The greatest emphasis has been placed on the $l=1$ transfers, where analyzing power systematics for many transitions establish a clear and strong dependence on Q value, in addition to the expected j dependence. In light of this strong Q dependence, spin assignments based on empirical comparisons of analyzing power data for $(\vec{d},t)$ transitions of appreciably different Q values are questionable. Although DWBA calculations generally fail to reproduce the measured analyzing powers quantitatively, they do at least exhibit qualitatively similar Q-dependent shifts in magnitude and in the phase of the oscillations in $iT_{11}(\theta)$.

The strong observed Q dependence and the quantitative inadequacy of the DWBA calculations hinder the analysis of analyzing power data for unresolved or mixed-j transitions. In those few cases where the analysis could be based upon empirical $iT_{11}(\theta)$ calibration curves drawn from measurements for single-j transitions of appropriate l, j, and Q values, we have demonstrated the usefulness of the analyzing power data in quantitative determinations of the relative contributions from different j values.

Despite the complications we have described, it is clear from the present work that the $(\vec{d},t)$ measurements are still quite useful for deducing values of the total angular momentum transfer. The present work has confirmed a number of previous spin and parity assignments to states in ^{67}Zn, ^{63}Ni, and ^{56}Fe, and has yielded new definite assignments of $\frac{3}{2}^-$ for the 2.149 MeV state in ^{63}Ni and $\frac{5}{2}^+$ for the 0.980 MeV state in ^{67}Zn.

This work was supported in part by the U.S. Department of Energy.

---

*Present address: Siemens Gammasonics, 2000 Nuclear Drive, Des Plaines, Illinois 60018.

†Present address: Department of Physics, Indiana University, Bloomington, Indiana 47405.

[1]T. J. Yule and W. Haeberli, Nucl. Phys. A117, 1 (1968); D. C. Kocher and W. Haeberli, *ibid.* A196, 225 (1972).

[2]D. C. Kocher and W. Haeberli, Nucl. Phys. A252, 381 (1975).

[3]H. S. Liers, R. D. Rathmell, S. E. Vigdor, and W. W. Haeberli, Phys. Rev. Lett. 26, 261 (1971).

[4]S. E. Vigdor, R. D. Rathmell, H. S. Liers, and W. Haeberli, Nucl. Phys. A210, 70 (1973).

[5]B. Mayer, H. E. Conzett, W. Dahme, D. G. Kovar, R. M. Larimer, and Ch. Leeman, Phys. Rev. Lett. 32, 1452 (1974).

[6]S. E. Vigdor and W. Haeberli, Nucl. Phys. A253, 55 (1975); S. E. Vigdor, *ibid.* A253, 75 (1975).

[7]S. E. Vigdor and H. S. Liers (unpublished).

[8]J. M. Lohr and W. Haeberli, Nucl. Phys. A232, 381 (1974).

[9]P. Schwandt and W. Haeberli, Nucl. Phys. A110, 585 (1968).

[10]P. Schwandt (private communication).

[11]F. D. Becchetti, Jr. and G. W. Greenlees, in *Proceedings of the Third International Symposium on Polarization Phenomena in Nuclear Reactions, Madison, 1970,* edited by H. H. Barschall and W. Haeberli (University of Wisconsin Press, Madison, 1971), p. 682.

[12]R. L. Auble, Nucl. Data Sheets 16, 417 (1975).

[13]R. L. Auble, Nucl. Data Sheets 14, 119 (1975).

[14]R. L. Auble, Nucl. Data Sheets 20, 253 (1977).

[15]J. R. Beene, Nucl. Data Sheets 25, 235 (1978).

[16]G. R. Satchler, Nucl. Phys. 55, 1 (1964).

[17]G. A. Huttlin, J. A. Aymar, J. A. Bieszk, S. Sen, and A. A. Rollefson, Nucl. Phys. A263, 445 (1976).

[18]M. E. Brandan and W. Haeberli, Nucl. Phys. A287, 205 (1977).

[19]J. A. Bieszk, L. Montestruque, and S. E. Darden, Phys. Rev. C 16, 1333 (1977).

[20]P. W. Keaton, Jr., *Proceedings of the Fourth International Symposium on Polarization Phenomena in Nuclear Reactions, Zürich, 1975,* edited by W. Grüebler and V. König (Birkhäuser, Basel, 1976), p. 173.

[21]R. A. Hardekopf, R. F. Haglund, Jr., G. G. Ohlsen, W. J. Thompson, and L. R. Veeser, Phys. Rev. C 21, 906 (1980).

[22]S. E. Vigdor, R. D. Rathmell, and W. Haeberli, Nucl. Phys. A210, 93 (1973).

[23]Computer Code DTCODE (unpublished).

[24]M. Borsaru, J. Nurzynski, D. W. Gebbie, C. L. Hollas, S. Whineray, N. H. Merrill, L. O. Barbopoulos, and A. R. Quinton, Nucl. Phys. A237, 93 (1975).

[25]E. K. Lin and B. L. Cohen, Phys. Rev. 132, 2632 (1963).

[26]D. von Ehrenstein and J. P. Schiffer, Phys. Rev. 164, 1374 (1967).

[27]H. A. Ismail, W. H. Moore, J. N. Hallock, and H. A. Enge, Phys. Rev. C 9, 1662 (1974).

[28]G. P. A. Berg and P. A. Quin, Nucl. Phys. A274, 141 (1976).

[29]W. W. Daehnick, Phys. Rev. 177, 1763 (1969).